JOURNAL OF GUIDANCE, CONTROL, AND DYNAMICS
Vol. 24, No. 4, July–August 2001

# Thrust Limited Coplanar Aeroassisted Orbital Transfer

Helge Baumann*
*University of Hamburg, D-20146 Hamburg, Germany*

**Two fuel-minimal aeroassisted orbital transfers are examined. Transfers from geosynchronous orbit to a low Earth orbit are considered. Instead of assuming an impulsive thrust on initial and final orbit, limited thrust on a nonvanishing interval on each orbit is introduced. In the atmospheric part, the transfer vehicle is controlled via the lift coefficient. The influence of Earth's rotation is considered also. Whereas in the atmospheric part an Earth-fixed frame of reference is used, the nonatmospheric parts are considered in an inertial frame of reference. This leads to an optimal control problem with well-defined jumps in the state and adjoint variables at the junction points between atmospheric and nonatmospheric arcs. The necessary conditions, including adjoint differential equations, boundary and interior point conditions, and control conditions, are derived to set up a boundary value problem. Solutions for a high and a low maximum magnitude of thrust with Earth's rotation, first neglected and later included, are presented.**

## Nomenclature

$C_D$ = drag coefficient
$C_L$ = lift coefficient
$D$ = drag
$g$ = local acceleration of gravity
$g_0$ = acceleration of gravity at sea level
$\mathcal{H}$ = Hamiltonian
$h$ = altitude
$h_a$ = altitude of the edge of the atmosphere
$h_c$ = normalized altitude of low Earth orbit (LEO)
$h_d$ = normalized altitude of geosynchronous Earth orbit (GEO)
$I_{sp}$ = specific impulse
$L$ = lift
$m$ = mass of the vehicle
$m_0$ = initial mass of the vehicle
$r$ = radius
$r_0$ = radius of Earth
$S$ = reference surface area
$T$ = thrust
$t_1$ = final time
$v$ = velocity
$v_c$ = normalized orbit velocity of LEO
$v_d$ = normalized orbit velocity of GEO
$\beta$ = reference altitude for density of atmosphere
$\gamma$ = path inclination
$\delta$ = normalized atmosphere density
$\zeta$ = normalized thrust
$\eta$ = normalized lift coefficient
$\lambda$ = adjoint variable
$\mu$ = Earth's gravitational constant
$\nu$ = Lagrange parameter
$\rho$ = atmosphere density
$\rho_0$ = reference atmosphere density
$\tau$ = switching or junction point
$\phi$ = switching function of control $\zeta$
$\psi$ = thrust angle of attack
$\omega$ = Earth's angular velocity

## Introduction

A COMMON task in space-travel problems is the change of orbits around the Earth or any other central mass with atmosphere. One important objective of orbit transfers is to minimize fuel consumption. Since the work of London,[1] it is well known that in certain maneuvers the additional use of aerodynamic forces in combination with propulsive forces is advantageous over an all-propulsive mode. This type of transfer using propulsive and atmospheric forces is called an aeroassisted orbital transfer (AOT).

To utilize aerodynamic forces, the trajectory is partially shifted into the Earth's atmosphere. Hence, the trajectory and transfer time are prolonged. Furthermore, to reach the atmosphere, fuel consumption on the initial orbit is increased. However, impulsive thrust at the final orbit and, therefore, overall fuel consumption is extensively reduced in comparison to pure propulsion transfers.

Surveys of the work that has been done so far are given by Walberg,[2] Mease,[3] and Miele.[4]

In general, by assuming impulsive thrusting, the problem is reduced to the atmospheric subarc.[5–9] Inside the atmosphere the AOT vehicle (AOTV) is controlled by the angle of attack or by the lift coefficient. In the literature, different control structures have been considered.[6,7] In this paper, a varied control structure is introduced.

Although mainly direct methods are used to solve AOT problems, indirect methods have been applied to AOT problems, for example, by Naidu[6] and Seywald.[10] Advantages are the high precision of the solution, the possibility to obtain detailed properties of the trajectory, and that the controls can be shown to satisfy the minimum principle. Therefore, an indirect method is used in this paper. On the downside of this method are that appropriate initial estimates for the states and the adjoints have to be provided.

In the majority of the earlier investigations, impulsive thrusting on the de- and reorbit has been considered. However, this case gives a high value of maximum magnitude of thrust. Given a limited value of thrust, intervals of thrust occur with an extension of a few seconds up to hours. First results of an AOT with low limited thrust have been presented recently.[11] In this paper these results are extended.

Taking into account Earth's rotation, the fuel-optimal AOT with high and low maximum magnitudes of thrust is considered. Because of the usage of different frames of reference inside and outside the atmosphere, an optimal control problem with discontinuities in the state variables at interior points is required.

The coplanar transfer treated in this paper is a basic one that can be adapted to other system data or elliptical orbits easily. It is also a starting point for the investigation of noncoplanar transfers, more important to real missions and analyzed in the impulsive formulation by various authors.[4,6,9,10,12,13] Recent results of noncoplanar transfers with limited thrust will be published elsewhere.

Furthermore, starting with the presented solutions, thermal constraints or other restrictions can be added. Feasible trajectories with respect to the constraints are obtained easily, whereas the identification of the optimal solution requires additional necessary conditions and extended control structures and, therefore, introduces major changes to the boundary value problem.

Received 28 March 2000; accepted for publication 6 September 2000. 

*Ph.D. Candidate, Department of Mathematics, Bundesstraße 55.

## General Optimal Control Problem

The resulting optimal control problems are of the following general type. Let $\boldsymbol{x}(\tau^-)$ and $\boldsymbol{x}(\tau^+)$ denote the left-hand and right-hand limit of $\boldsymbol{x}$ at $t=\tau$, respectively. Furthermore, let $0=:\tau_0<\tau_1,\ldots,\tau_N:=t_1$, a partition of the interval $[0,t_1]$.

The general problem (GP) is solved as follows: Determine piecewise continuous functions $\boldsymbol{u}$, piecewise continuously differentiable functions $\boldsymbol{x}$ and $\tau_1,\ldots,\tau_{N-1}$, and $t_1$ such that

$$I=g[\boldsymbol{x}(t_1)] \tag{1}$$

is minimized, subject to the conditions

$$\frac{\mathrm{d}\boldsymbol{x}}{\mathrm{d}t}=\boldsymbol{f}[\boldsymbol{x}(t),\boldsymbol{u}(t),t], \qquad t\in(\tau_{j-1},\tau_j), \qquad j=1,\ldots,N$$

$$\boldsymbol{\Psi}^0[\boldsymbol{x}(t_0)]=0, \qquad \boldsymbol{\Psi}^N[x(t_1),t_1]=0$$

$$\boldsymbol{\Psi}^j\left[\boldsymbol{x}\left(\tau_j^-\right),\boldsymbol{x}\left(\tau_j^+\right),\tau_j\right]=0, \qquad j=1,\ldots,N-1$$

$$\boldsymbol{u}(t)\in U:=\left\{\boldsymbol{u}\in\boldsymbol{R}^m\,\middle|\,c_i(u)\le 0, i=1,\ldots,s\right\} \tag{2}$$

where $t\in\boldsymbol{R}$, $\boldsymbol{x}(t)\in\boldsymbol{R}^n$, and $\boldsymbol{u}(t)\in\boldsymbol{R}^m$ are time, state vector, and control vector, respectively. Note that $\boldsymbol{x}$ and $\boldsymbol{f}$ might be discontinuous in $\tau_1,\ldots,\tau_{N-1}$. The set of admissible controls $U$ is assumed to be nonempty, closed, and convex. The functions $g:\boldsymbol{R}^n\to\boldsymbol{R}$, $\boldsymbol{\Psi}^0:\boldsymbol{R}^n\to\boldsymbol{R}^{k_0}$, $\boldsymbol{\Psi}^j:\boldsymbol{R}^{2n+1}\to\boldsymbol{R}^{k_j}$, $j=1,\ldots,N-1$, $\boldsymbol{\Psi}^N:\boldsymbol{R}^{n+1}\to\boldsymbol{R}^{k_N}$, $\boldsymbol{c}:\boldsymbol{R}^{m+1}\to\boldsymbol{R}^s$, and $\boldsymbol{f}:\boldsymbol{R}^n\times\boldsymbol{R}^m\times[0,t_1]\to\boldsymbol{R}^n$ on each subinterval $(\tau_{j-1},\tau_j)$, $j=1,\ldots,N$, are assumed to be sufficiently smooth with respect to all of their arguments. The junction times $\tau_1,\ldots,\tau_{N-1}$ and the final time $t_1$ are variable. The Hamiltonian is defined by introducing Lagrange multiplier functions $\boldsymbol{\lambda}:[0,t_1]\to\boldsymbol{R}^n$ as

$$\mathcal{H}:=\boldsymbol{\lambda}^T\boldsymbol{f} \tag{3}$$

Furthermore, define

$$G:=g+\sum_{j=0}^{N}[\boldsymbol{\nu}^j]^T\boldsymbol{\Psi}^j$$

with $N+1$ constant Lagrange multipliers $\boldsymbol{\nu}^j\in\boldsymbol{R}^{k_j}$, $j=0,\ldots,N$.

If $(\boldsymbol{x}^*,\boldsymbol{u}^*,\tau_1,\ldots,\tau_N)$ is a regular solution of the optimal control problem GP, the following necessary conditions have to be satisfied,[14]

$$\left(\frac{\mathrm{d}\boldsymbol{\lambda}}{\mathrm{d}t}\right)^T=-\frac{\partial\mathcal{H}}{\partial\boldsymbol{x}}, \qquad \tau_{j-1}<t<\tau_j \tag{4}$$

$$\boldsymbol{\lambda}\left(\tau_{j-1}^+\right)^T=-\frac{\partial G}{\partial\boldsymbol{x}}\left(\tau_{j-1}^+\right), \qquad \boldsymbol{\lambda}\left(\tau_j^-\right)^T=\frac{\partial G}{\partial\boldsymbol{x}}\left(\tau_j^-\right) \tag{5}$$

with $j=1,\ldots,N$.

In addition, the necessary conditions for the Hamiltonian read

$$\frac{\partial G}{\partial\tau_j}+\mathcal{H}\left[\tau_j^-\right]-\mathcal{H}\left[\tau_j^+\right]=0, \qquad j=1,\ldots,N-1 \tag{6}$$

$$\frac{\partial G}{\partial t_1}+\mathcal{H}\left[t_1^-\right]=0 \tag{7}$$

Finally, at each instant of time, the optimal control $\boldsymbol{u}^*$ satisfies Pontryagin's minimum principle, that is,

$$\boldsymbol{u}^*(t)=\underset{\boldsymbol{u}\in U}{\arg\min}\,\mathcal{H}[\boldsymbol{x}^*(t),\boldsymbol{u},\boldsymbol{\lambda}(t),t] \tag{8}$$

## Statement of the Problem

The problem of fuel-optimal transfer from geosynchronous Earth orbit (GEO) to low Earth orbit (LEO) with a single atmospheric pass is treated. The initial and final orbits are both assumed to be circular and equatorial. Hence, the transfer takes place in one common plane. The altitude of LEO, 350 km, may approximate the orbit altitude of the International Space Station.

In the equatorial plane, Earth's surface is considered circular, with radius $r_0=6378$ km and with a central gravitational field governed by the inverse square law. First, the nonrotating case problem P1 is investigated. Second, Earth's rotation is included (problem P2). To demonstrate the effects of rotation terms, a precise model with Coriolis and transport acceleration terms was implemented. The atmosphere is treated as fixed with regard to Earth.

The density of the atmosphere is postulated as exponentially decreasing. Other models, for example, piecewise exponentially decreasing density, also could be implemented but imply the usage of additional switching points and the determination of additional update parameters to the adjoints. Therefore, we prefer the simple model. The boundary of the atmosphere is set to altitude $h=h_a=120$ km. For altitudes $h>h_a$, air density is set equal to zero, that is,

$$\rho=\rho(h)=\begin{cases}\rho_0\exp(-h\beta), & \text{if} \quad h\le h_a\\ 0, & \text{if} \quad h>h_a\end{cases} \tag{9}$$

with constants $\rho_0$ and $\beta$.

The AOTV[6,7,15] has a moderate lift-to-drag capability of about 1.5. The lift coefficient $C_L$ is bounded in absolute value to be less than or equal to 0.9. The values for mass and reference surface area are chosen to approximate a mass-to-surface area of 300 kg/m$^2$ inside the atmosphere. Different upper bounds of maximum thrust will be considered to show the interdependency between maximum thrust and trajectory as well as fuel consumption. The direction of thrust is not fixed with respect to the vehicle. It is determined by the thrust angle $\psi$, which describes the angle between velocity and thrust vectors.

### Equations of Motion

The equations of motion with respect to the rotating Earth are given by

$$\frac{\mathrm{d}h}{\mathrm{d}t}=v\sin\gamma$$

$$\frac{\mathrm{d}v}{\mathrm{d}t}=\frac{T}{m}\cos\psi-\frac{\left(C_{D0}+C_{D2}C_L^2\right)\rho v^2S}{2m}-g\sin\gamma+\omega^2r\sin\gamma$$

$$\frac{\mathrm{d}\gamma}{\mathrm{d}t}=\frac{T\sin\psi}{mv}+\frac{C_L\rho v^2S}{2mv}+\left(\frac{v}{r}-\frac{g}{v}\right)\cos\gamma+2\omega+\omega^2\cos\gamma\frac{r}{v}$$

$$\frac{\mathrm{d}m}{\mathrm{d}t}=-\frac{T}{g_0I_{\mathrm{sp}}} \tag{10}$$

with $g=\mu/r^2$, $g_0=\mu/r_0^2$, and $r=r_0+h$. The aerodynamic forces drag and lift are expressed in terms of the lift coefficient $C_L$, where a quadratic polar is assumed with the constants $C_{D0}$ and $C_{D2}$. The dependency of the aerodynamic coefficients on the Mach number and the Reynolds number is neglected.

### Normalized System

For numerical reasons the state variables are scaled in the following way[6,16]:

$$\bar{h}(\bar{t}):=h(a\bar{t})/h_a, \qquad \bar{v}(\bar{t}):=av(a\bar{t})/r_a$$

$$\bar{\gamma}:=\gamma(a\bar{t}), \qquad \bar{m}(\bar{t}):=m(a\bar{t})/m_0 \tag{11}$$

with $\bar{t}:=t/a$ and $a:=\sqrt{(r_a^3/\mu)}$.

Also, new normalized control variables are introduced with

$$\eta:=C_L/K, \qquad \zeta:=Tr_a^2\big/\mu m_0 \tag{12}$$

and constant $K:=\sqrt{(C_{D0}/C_{D2})}$. Therefore, the scaled control constraints read

$$C_{L_{\min}}\big/K:=\eta_{\min}\le\eta\le\eta_{\max}:=C_{L_{\max}}\big/K$$

$$0\le\zeta\le\zeta_{\max}:=T_{\max}r_a^2\big/\mu m_0 \tag{13}$$

With the abbreviations

$$A_1 := 0.5C_{D0}\rho_0 r_a S/m_0, \qquad A_2 := 0.5K\rho_0 r_a S/m_0$$

$$A_3 := \sqrt{\mu/r_a}\,/(g_0 I_{sp}), \qquad A_4 := -\beta h_a, \qquad \tilde{\omega} := \omega a$$

$$b := r_a/h_a, \qquad c(h) := b - 1 + h \tag{14}$$

$$\delta(\bar{h}) := \rho(h)/\rho_0 = \begin{cases} \exp(\bar{h}A_4), & \text{if} \quad \bar{h} \le 1 \\ 0, & \text{if} \quad \bar{h} > 1 \end{cases} \tag{15}$$

and omission of the bars for simplicity, the normalized equations of motions are given by

$$\frac{\mathrm{d}h}{\mathrm{d}t} = bv\sin\gamma$$

$$\frac{\mathrm{d}v}{\mathrm{d}t} = \frac{\zeta\cos\Psi}{m} - \frac{A_1(1+\eta^2)\delta(h)v^2}{m} - \frac{b^2\sin\gamma}{c(h)^2} + \frac{\tilde{\omega}^2 c(h)\sin\gamma}{b}$$

$$\frac{\mathrm{d}\gamma}{\mathrm{d}t} = \frac{\zeta\sin\psi}{mv} + \frac{A_2\eta\delta(h)v^2}{m} + \frac{\tilde{\omega}^2 c(h)\cos\gamma}{bv} + \left[v - \frac{b}{c(h)v}\right]\frac{b\cos\gamma}{c(h)} + 2\tilde{\omega}$$

$$\frac{\mathrm{d}m}{\mathrm{d}t} = -\zeta A_3 \tag{16}$$

**Boundary and Interior Point Conditions**

Initial and final altitude is prescribed by the altitude of high Earth orbit (HEO) and LEO, respectively. At these points the velocity has to match the orbit velocity on HEO and LEO, respectively. To stay on the circular HEO or LEO, the flight-path angle vanishes at the beginning and at the end. The initial mass is fixed and the final mass is to be maximized:

$$h(0) = h_d, \qquad v(0) = v_d, \qquad \gamma(0) = 0, \qquad m(0) = 1$$

$$v(t_1) = v_c, \qquad \gamma(t_1) = 0, \qquad h(t_1) = h_c \tag{17}$$

The discontinuity of air density, Eqs. (9) and (15), at the atmospheric boundary yields discontinuities of the system equations at interior points. Although the discontinuity is small, it is nevertheless taken into account for a proper numerical treatment of the boundary value problem, especially for a numerical check of the necessary conditions. Therefore, the transfer is subdivided into atmospheric and nonatmospheric parts. This yields the structure shown in Fig. 1.

The switching points $\tau_e$ and $\tau_f$ are determined by the interior point conditions

$$\Psi_1^1 = h(\tau_e) - 1 = 0, \qquad \Psi_1^2 = h(\tau_f) - 1 = 0 \tag{18}$$

corresponding to the distinction in Eq. (15). The right-hand side of Eq. (16) remains continuously differentiable in each of the three parts.

**Problem P1**

The fuel consumption of the transfer is given by the difference of initial and final mass, $m(0) - m(t_1)$. Because of the constant initial mass, the cost function is set to

$$g[x(t_1)] = -m(t_1) \tag{19}$$

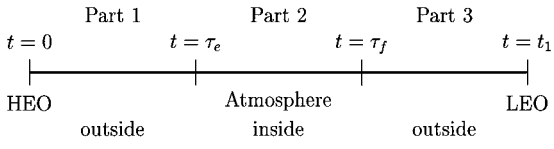


**Fig. 1 Subdivision of AOT.**

In this problem, the influence of Earth's rotation is neglected, that is, $\tilde{\omega} = 0$ in Eq. (16). At the junction points the continuity conditions hold

$$\Psi_2^1 = h(\tau_e^+) - h(\tau_e^-) = 0, \qquad \Psi_2^2 = h(\tau_f^+) - h(\tau_f^-) = 0$$

$$\Psi_3^1 = v(\tau_e^+) - v(\tau_e^-) = 0, \qquad \Psi_3^2 = v(\tau_f^+) - v(\tau_f^-) = 0$$

$$\Psi_4^1 = \gamma(\tau_e^+) - \gamma(\tau_e^-) = 0, \qquad \Psi_4^2 = \gamma(\tau_f^+) - \gamma(\tau_f^-) = 0$$

$$\Psi_5^1 = m(\tau_e^+) - m(\tau_e^-) = 0, \qquad \Psi_5^2 = m(\tau_f^+) - m(\tau_f^-) = 0 \tag{20}$$

Problem P1 can be stated as follows. Determine functions $\boldsymbol{u} := (\eta, \zeta, \psi)^T$ and $\boldsymbol{x} := (h, v, \gamma, m)^T$ as well as switching points $\tau_e$ and $\tau_f$ to minimize

$$I := -m(t_1)$$

subject to the system equations (16) with $\tilde{\omega} = 0$, the boundary conditions (17) the interior point conditions (18) and (20), and the control constraints

$$c_1(\eta, \zeta) := \eta_{\min} - \eta \le 0, \qquad c_2(\eta, \zeta) := \eta - \eta_{\max} \le 0$$

$$c_3(\eta, \zeta) := \zeta_{\min} - \zeta \le 0, \qquad c_4(\eta, \zeta) := \zeta - \zeta_{\max} \le 0 \tag{21}$$

Problem P1 is considered twice, with P1a a rather high and P1b a low value of $\zeta_{\max}$.

**Problem P2**

In problem P2, the effect of Earth's rotations is also taken into account. Transforming the boundary conditions to an Earth-fixed frame of reference yields the inital condition $v(0) = 0$. Numerical difficulties in the differential equations (16) arise. On the other hand, staying in the inertial frame of reference implies transforming the aerodynamic forces at each instant of time. Therefore, we stay for the nonatmospheric parts in the inertial frame of reference, that is, Eqs. (16) with $\tilde{\omega} = 0$, and we keep the old boundary conditions (17). At the two junction points the variables are updated to the Earth-fixed frame of reference by fulfilling conditions (22). The trajectory in the atmospheric part is computed in the Earth-fixed frame of reference by Eqs. (16).

At the junction points the two states, altitude and mass, remain continuous, whereas velocity and flight-path angle are updated subject to the conditions

$$\psi_3^1 = v(\tau_e^+)\cos\gamma(\tau_e^+) - v(\tau_e^-)\cos\gamma(\tau_e^-) + \tilde{\omega}c(h)/b = 0$$

$$\psi_4^1 = v(\tau_e^+)\sin\gamma(\tau_e^+) - v(\tau_e^-)\sin\gamma(\tau_e^-) = 0$$

$$\psi_3^2 = v(\tau_f^+)\cos\gamma(\tau_f^+) - v(\tau_f^-)\cos\gamma(\tau_f^-) - \tilde{\omega}c(h)/b = 0$$

$$\psi_4^2 = v(\tau_f^+)\sin\gamma(\tau_f^+) - v(\tau_f^-)\sin\gamma(\tau_f^-) = 0 \tag{22}$$

Problem P2 is stated as follows. Determine functions $\boldsymbol{u} := (\eta, \zeta, \psi)^T$ and $\boldsymbol{x} := (h, v, \gamma, m)^T$ as well as switching points $\tau_e$ and $\tau_f$ to minimize

$$I := -m(t_1)$$

subject to the system equations (16) in $[0, \tau_e)$, $(\tau_f, t_1]$ with $\tilde{\omega} = 0$, in $[\tau_e, \tau_f]$ with $\tilde{\omega} = \omega a = 0.060502746$, the boundary conditions (17), the interior point conditions (18) and (22), and the control constraints (21). Like problem P1, problem P2 is considered twice, with P2a a high and P2b a low value of $\zeta_{\max}$.

**Necessary Conditions**

Applying the necessary conditions stated in Eqs. (3–8) to the optimal control problems, one obtains the adjoint differential equations

$$\frac{\mathrm{d}\lambda_h}{\mathrm{d}t} = -\lambda_v\left[-\frac{A_1(1+\eta^2)\delta(h)A_4v^2}{m} + \frac{2\sin\gamma b^2}{c(h)^3} + \frac{\sin\gamma\tilde{\omega}^2}{b}\right] - \lambda_\gamma\left\{\frac{A_2\eta\delta(h)A_4v}{m} + \frac{\cos\gamma\tilde{\omega}^2}{bv} + \left[-v + \frac{2b}{c(h)v}\right]\frac{\cos\gamma b}{c(h)^2}\right\}$$

$$\frac{\mathrm{d}\lambda_v}{\mathrm{d}t} = -\lambda_h b\sin\gamma + \frac{2\lambda_v A_1(1+\eta^2)\delta(h)v}{m} - \lambda_\gamma\left\{\frac{-\zeta\sin\psi}{mv^2} + \frac{A_2\eta\delta(h)}{m} + \left[1 + \frac{b}{c(h)v^2}\right]\frac{\cos\gamma b}{c(h)} - \frac{\tilde{\omega}^2\cos\gamma c(h)}{bv^2}\right\}$$

$$\frac{\mathrm{d}\lambda_\gamma}{\mathrm{d}t} = -\lambda_h bv\cos\gamma - \lambda_v\left[\frac{-b^2}{c(h)^2\cos\gamma} + \frac{\tilde{\omega}^2\cos\gamma c(h)}{b}\right] + \lambda_\gamma\left[v - \frac{b}{c(h)v}\right]\frac{\sin\gamma b}{c(h)} + \frac{\tilde{\omega}^2\sin\gamma c(h)}{bv}$$

$$\frac{\mathrm{d}\lambda_m}{\mathrm{d}t} = \lambda_v\left[\frac{\zeta\cos\psi}{m^2} - \frac{A_1(1+\eta^2)\delta(h)v^2}{m^2}\right] + \lambda_\gamma\left[\frac{\zeta\sin\psi}{m^2v} + \frac{A_2\eta\delta(h)v}{m^2}\right] \tag{23}$$

and the natural boundary conditions

$$\lambda_m(t_1) = -1, \qquad \mathcal{H}(t_1) = 0 \tag{24}$$

In view of the continuous states at the junction points in problem P1, Eq. (5) yields the continuity of the adjoints $\lambda_v$, $\lambda_\gamma$, and $\lambda_m$. In the case of the altitude, Eqs. (18) also have to be considered in addition to the continuity of $h$. Applying Eqs. (5) to the altitude at the junction points yields the update formulas

$$\lambda_h\left(\tau_e^+\right) = \lambda_h\left(\tau_e^-\right) - \nu^e, \qquad \lambda_h\left(\tau_f^+\right) = \lambda_h\left(\tau_f^-\right) - \nu^f \tag{25}$$

The multipliers $\nu^e$ and $\nu^f$ are determined by Eq. (6), that is,

$$\mathcal{H}[\tau^+] = \mathcal{H}[\tau^-], \qquad \tau = \tau_e, \tau_f \tag{26}$$

In problem P2, velocity and flight-path angle are discontinuous at the junction points. Therefore, update formulas for the corresponding adjoints have to be derived. The interior point conditions (22) are applied to Eqs. (5). This yields the following update conditions for the adjoint variables

$$\lambda_v(\tau^+) = \lambda_v(\tau^-)[\sin\gamma(\tau^+)\sin\gamma(\tau^-) + \cos\gamma(\tau^+)\cos\gamma(\tau^-)] + \lambda_\gamma(\tau^-)/v(\tau^-)[\cos\gamma(\tau^-)\sin\gamma(\tau^+) - \sin\gamma(\tau^-)\cos\gamma(\tau^+)]$$

$$\lambda_\gamma(\tau^+) = \lambda_v(\tau^-)v(\tau^+)[\sin\gamma(\tau^-)\cos\gamma(\tau^+) - \cos\gamma(\tau^-)\sin\gamma(\tau^+)] + \lambda_\gamma(\tau^-)v(\tau^+)/v(\tau^-)[\cos\gamma(\tau^+)\cos\gamma(\tau^-) + \sin\gamma(\tau^-)\sin\gamma(\tau^+)] \tag{27}$$

with $\tau = \tau_e, \tau_f$.

To handle the free final time $t_1$, the domain of the differential equations is transformed linearly to the unit interval. Consequently, $\bar{\tau}_e = \tau_e/t_1$ and $\bar{\tau}_f = \tau_f/t_1$ are the scaled switching points. Once again, for simplicity, the bars are dropped.

#### Control Functions

The control functions are determined by the minimum principle Eq. (8).

Inside the atmosphere, the Hamiltonian is a quadratic function with respect to $\eta$. If the parabola is directed upward, that is, $\lambda_v < 0$, a unique minimum exists. This is not true in the case $\lambda_v \geq 0$. However, because $\eta$ is bounded from above and below, a feasible minimum exists. In detail, $\eta$ is determined by the following rules. First, an unbounded control $\eta_{\text{free}}$ is computed by

$$\eta_{\text{free}} = \lambda_\gamma \Big/ \left(2\lambda_v v\sqrt{C_{D0}C_{D2}}\right) \tag{28}$$

This condition arises from the necessary condition of unconstrained controls $\partial\mathcal{H}/\partial\eta = 0$. Second, the constraints are taken into account by setting

$$\eta = \eta_{\text{free}}, \quad \text{if} \quad \lambda_v < 0, \quad \eta_{\min} \leq \eta_{\text{free}} \leq \eta_{\max}$$

$$\eta = \eta_{\min}, \quad \text{if} \quad \begin{cases} \lambda_v < 0, & \eta_{\text{free}} < \eta_{\min} \\ \lambda_v > 0, & \eta_{\text{free}} \geq (\eta_{\min} + \eta_{\max})/2 \\ \lambda_v = 0, & \lambda_\gamma > 0 \end{cases}$$

$$\eta = \eta_{\max}, \quad \text{if} \quad \begin{cases} \lambda_v < 0, & \eta_{\text{free}} > \eta_{\max} \\ \lambda_v > 0, & \eta_{\text{free}} < (\eta_{\min} + \eta_{\max})/2 \\ \lambda_v = 0, & \lambda_\gamma < 0 \end{cases}$$

The Hamiltonian is linear in the normalized magnitude of thrust $\zeta$. As it turns out, $\zeta$ is a bang–bang control characterized by the switching function

$$\phi := \frac{\partial\mathcal{H}}{\partial\zeta} = \frac{\lambda_v\cos\psi}{m} + \frac{\lambda_\gamma\sin\psi}{mv} - \lambda_m A_3 \tag{29}$$

and determined by

$$\zeta = \begin{cases} \zeta_{\max}, & \text{if} \quad \phi < 0 \\ 0, & \text{if} \quad \phi > 0 \end{cases} \tag{30}$$

The third control function is the unconstrained thrust angle of attack $\psi$. Here the minimum principle demands $\partial\mathcal{H}/\partial\psi = 0$ and $\partial^2\mathcal{H}/\partial\psi^2 \geq 0$. This yields

$$\sin\psi = \frac{-\lambda_\gamma}{\sqrt{\lambda_v^2v^2 + \lambda_\gamma^2}}, \qquad \cos\psi = \frac{-\lambda_v v}{\sqrt{\lambda_v^2v^2 + \lambda_\gamma^2}} \tag{31}$$

#### Boundary Value Problem (BVP)

The multipoint boundary value problems (BVPs) consist of the eight differential equations (16) and (23), linearly transformed by $t_1$. In BVP1, corresponding to problem P1, as well as in the nonatmospheric parts of BVP2, correspondinging to problem P2, $\tilde{\omega} = 0$ holds. To the BVPs belong five parameters, $\tau_e$, $\tau_f$, $t_1$, $\nu^e$, and $\nu^f$. The nine boundary and four interior point conditions are given by Eqs. (17) and (24), as well as Eqs. (18) and (26). At junction points in BVP1, only the adjoint variable $\lambda_h$ has to be updated via Eq. (25). In BVP2, the states are updated subject to Eqs. (22) at the junction points and the adjoints by Eqs. (27). The control is determined by the rules (28–31).

## Results

The multipoint BVPs, BVP1 and BVP2, corresponding to the optimal control problems P1 and P2, were solved with the implementation of the multiple shooting code BNDSCO.[17–19] To apply BNDSCO to the BVP, the control structure has to be provided by the user. The multiple shooting code returned results with a relative error of $10^{-8}$.

#### Control Structure

The control structure describes the number and relative position of constrained and free arcs of each control variable. The different arcs are separated by switching points $\tau_i$, which are determined by a switching condition.

The switching condition for the thrust $\zeta$ depends on the switching function $\phi$ and can easily be obtained from Eq. (30), that is, $\phi = 0$. The control structure maximal–minimal–maximal for $\zeta$ is assumed. Hence, no propulsion inside the atmosphere is predicted. A posteriori, by considering the switching function, it can be verified that this estimation leads to a trajectory satisfying the minimum principle.

In the case of the normalized lift coefficient $\eta$, the necessary conditions state that the control $\eta$ is continuous at the switching points. Therefore, as switching conditions, $\eta_{\text{free}} = \eta_{\min}$ or $\eta_{\text{free}} = \eta_{\max}$ are possible.

Various control structures with regard to the lift coefficient inside the atmosphere have been suggested in the literature, for example, $\eta \equiv \eta_{\min}$ (Ref. 7) or $\eta$: free–minimal–free.[15] However, applied to the problems P1 and P2, these control structures turn out to fail the necessary conditions. In the case of problem P1, this is discussed in detail in a previous work.[11] Note that the different control structures of the lift coefficient only yield small changes in the cost function. For real applications, other issues, for example, the robustness of the control structure, also have to be considered. In this paper, the control structure minimal-free for $\eta$ inside the atmosphere is assumed.

The different control parts are separated by switching points $\tau_{\zeta_1}, \tau_{\zeta_2}$, and $\tau_\eta$. Note that the junction points between the atmospheric and nonatmospheric parts, $\tau_e$ and $\tau_f$, are switching points too. A complete list of all switching points with their switching conditions is presented in Table 1.

**Table 1 All switching points with their switching conditions**

| Switching point | Switching conditions |
|---|---|
| $\tau_{\zeta_1}$ | $\phi = 0$ |
| $\tau_e$ | $h(\tau_e) = 1$ |
| $\tau_\eta$ | $\eta_{\min} = \eta_{\text{free}}$ |
| $\tau_f$ | $h(\tau_f) = 1$ |
| $\tau_{\zeta_2}$ | $\phi = 0$ |

**Table 2 Listing of the unscaled constants used in the numerical experiments.**

| Parameter | Value | Parameter | Value | Parameter | Value |
|---|---|---|---|---|---|
| $h_d$ | 35,786 km | $C_{L_{\min}}$ | −0.9 | $\rho_0$ | 1.225 kg/m$^3$ |
| $h_c$ | 350 km | $C_{L_{\max}}$ | 0.9 | $\mu$ | 3.986 $10^5$ km$^3$/s$^2$ |
| $h_a$ | 120 km | $C_{D0}$ | 0.1 | $\beta$ | 1/6,900 1/m |
| $r_0$ | 6,378 km | $C_{D2}$ | 1.11 | $m_0$ | 15,642.24 kg |
| $S$ | 36.2874 m$^2$ | $I_{\text{sp}}$ | 420 s | $\omega$ | 7.292462 $10^{-5}$ rad/s |
| $T^{\text{a}}_{\max}$ | $1.2 \times 10^6$ N | | | $T^{\text{b}}_{\max}$ | $5 \times 10^3$ N |

[a]Problems P1a and P2a. [b] Problems P1b and P2b.

## Numerical Results

The data used in the numerical calculations are listed in Table 2. Each of the problems P1 and P2 was calculated with the values $T_{\max} = 1.2 \times 10^6$ N (P1a and P2a) and $T_{\max} = 5 \times 10^3$ N (P1b and P2b). The rather high value of P1a and P2a was chosen to approximate the impulsive case. The duration of the reorbit thrusting phase in scaled time is less than $3 \times 10^{-5}$, that is, less than 0.7 s, cf. Table 3. This comes close to the impulsive thrust case. Of course, the deorbit thrust phase is longer, about 17 s.

As opposed to this rather high value, $T_{\max} = 5 \times 10^3$ N was chosen rather low to demonstrate the effect of limited thrust to the trajectory.

The starting point for the numerical calculations was a solution of the AOT problem with impulsive thrust obtained from previous results.[11] These results served as the initial estimation to the multiple shooting code for problem P1a. Continuation techniques were used to decrease the thrust limit to solve problem P1b.

Subsequently, the rotation terms were included. By application of continuation techniques, increasing the value of $\tilde{\omega}$ turns problem P1 into P2.

Figures 2–5 show the results of the computations with full Earth's rotation, but different values of maximum thrust. In comparison, Fig. 6 shows a part of the trajectory with rotation terms included and excluded. Key parameters of the solutions are listed in Table 3.

The history of the state variables of problem P2 is shown in Fig. 2. Because of the change of coordinate system, discontinuities occur with respect to velocity and flight-path angle at $t = \tau_e = 0.84077939$ and $t = \tau_f = 0.91100565$, the junction points between inside and outside the atmosphere. The discontinuities in the flight-path angle are too small to be seen; however, these points are marked by

**Table 3 Numerical results of the different problems**

| | Problem | | | |
|---|---|---|---|---|
| Parameter | P1a | P1b | P2a | P2b |
| $T_{\max}$, N | $1.2 \times 10^6$ | $5 \times 10^3$ | $1.2 \times 10^6$ | $5 \times 10^3$ |
| Initial mass, kg | 15,642.00 | 15,642.00 | 15,642.00 | 15,642.00 |
| Final mass, kg | 10,693.83 | 10,683.58 | 10,692.99 | 10,682.74 |
| Consumption, kg | 4,948.41 | 4,958.66 | 4,949.25 | 4,959.50 |
| Time of first thrusting, s | 16.30 | 3,919.69 | 16.30 | 3,919.84 |
| Time inside atmosphere, s | 1,728.13 | 1,728.21 | 1,736.70 | 1,736.78 |
| Time of second thrusting, s | 0.67 | 161.74 | 0.68 | 162.28 |
| Total time, s | 22,616.85 | 24,731.87 | 22,615.85 | 24,731.22 |

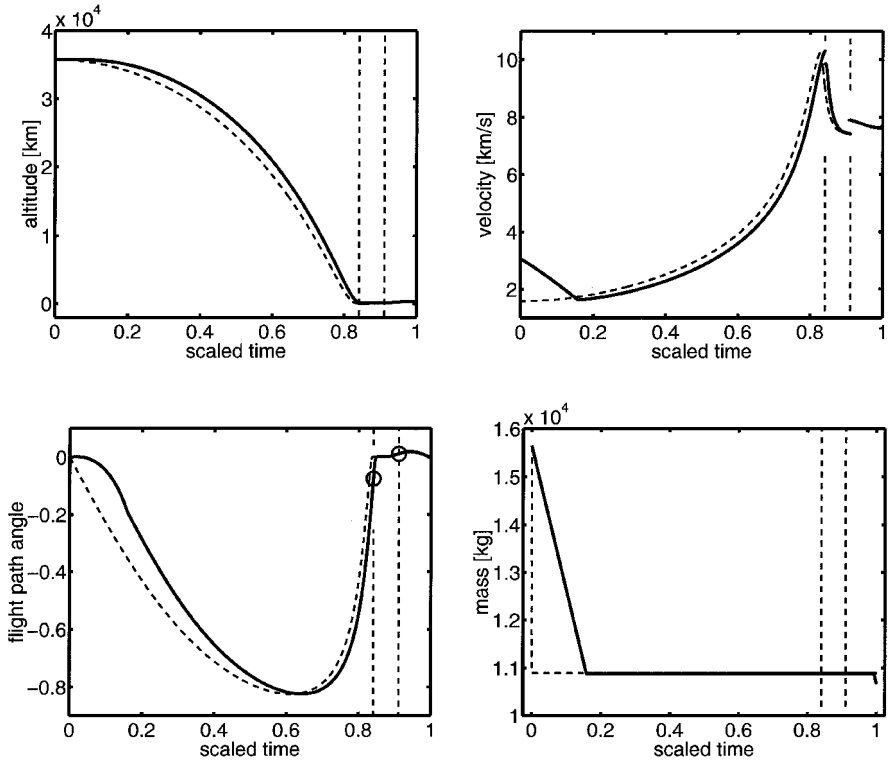


**Fig. 2 State variable history of the complete AOT: dashed line marks the solution for problem P2a, solid line the solution for problem P2b, and vertical dashed lines mark the boundary of the atmospheric part of problem P2b.**

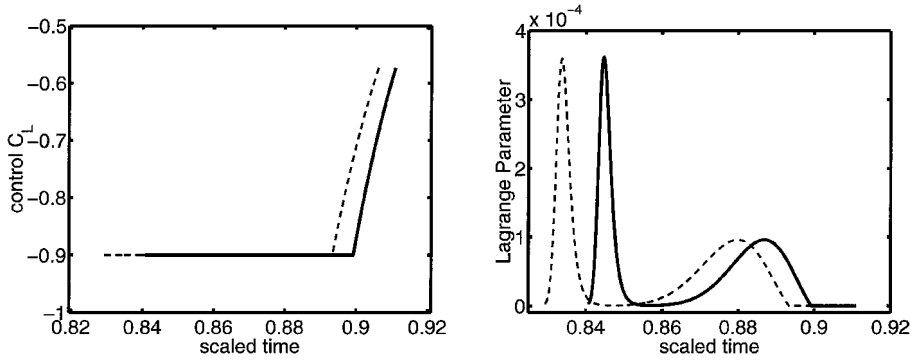


**Fig. 3 History of the lift coefficient $C_L$ and of $H_\eta$ in the atmospheric subarc: dashed line marks the solution of problem P2a and solid line the solution of problem P2b.**

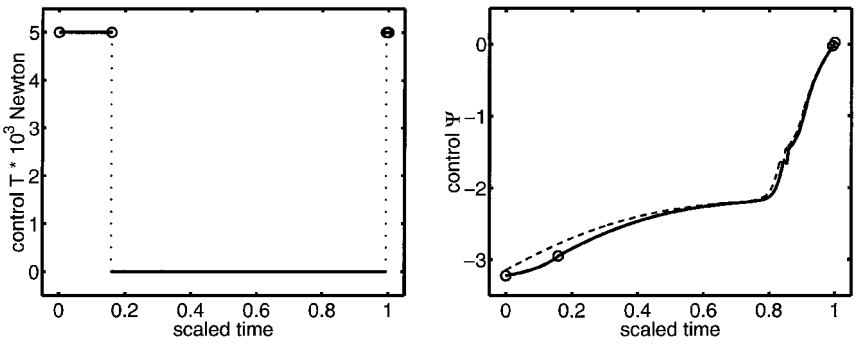


**Fig. 4 Histories of the magnitude of thrust and the thrust angle Ψ: circles mark the junction of thrusting and nonthrusting subarcs.**

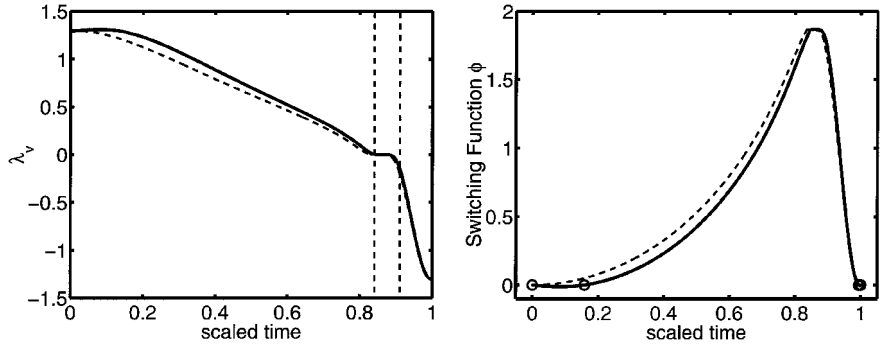


**Fig. 5 Time history of adjoint $\lambda_v$ and of the switching function: dashed line marks the solution of problem P2a, solid line the solution of problem P2b, vertical dashed lines the boundary of the atmospheric part of problem P2b, and circles the zeros of the switching function.**

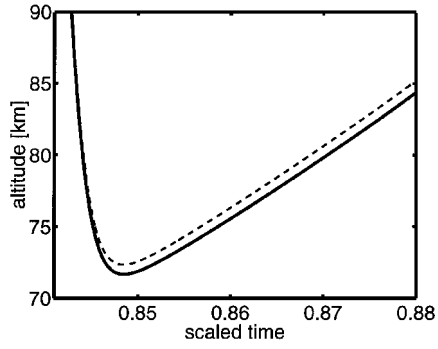


**Fig. 6 Part of the altitude history: dashed line marks the solution of problem P1b exclusive, solid line the solution of problem P2b inclusive of Earth's rotation terms.**

circles. Also, the sharp corner inside the atmosphere is a continuous differentiable part where the vehicle flattens out the steep dive and starts climbing moderately.

Because the transfer takes place in eastward direction, that is, in direction of Earth's rotation, the velocity with respect to Earth is less than with respect to the inertial system. Because of the use of different frames of reference, the atmospheric part of the velocity history seems to be shifted downward in Fig. 2.

Also from Fig. 2, it can be established that the vehicle equiped with a high maximum thrust almost immediately decreases altitude, whereas in the second case, the vehicle remains some time near HEO altitude. In fact, the initial thrust angle, $\Psi(0) = -3.22124659$, is less than $-\pi$, that is, the thrust vector decreases velocity and additionally pushes the vehicle slightly upward. This extends the trajectory. The history of the thrust angle is shown in Fig. 4.

The extension of the trajectory increases the total time of the transfer by 35:15 min:s. However, the time inside the atmosphere remains nearly constant.

With the results of problems P1 and P2 (Table 3), it is seen that the thrusting phases as well as the total time of the transfer have not changed significantly. The fuel consumption is very slightly increased, by less then 1 kg. Therefore, the inclusion of rotation terms has marginal effects on the nonatmospheric parts.

The time inside the atmosphere increases by approximately 8 s. In Fig. 6, a part of the altitude history inside the atmosphere is shown. Including rotation terms forces the AOTV to attain a lower minimum altitude.

The increment in fuel consumption may be expected for the following reason. In problem P2, the velocity of the AOTV with respect to the atmosphere is smaller than in problem P1 because the transfer takes place in direction of Earth's rotation. Therefore, the vehicle has to dip deeper into the atmosphere to produce adequate aerodynamic forces (Fig. 6). Consequently, at atmospheric entry and

**Table 4 Switching points with respect to the unit interval and initial values of adjoint variables for the problem P2b**

| Parameter | Initial values |
|---|---|
| *Switching points* | |
| $\tau_{\zeta_1}$ | 0.15849770 |
| $\tau_e$ | 0.84077939 |
| $\tau_\eta$ | 0.89921964 |
| $\tau_f$ | 0.91100565 |
| $\tau_{\zeta_2}$ | 0.99343836 |
| *Adjoint variables* | |
| $\lambda_h(0)$ | $0.68915719\times 10^{-3}$ |
| $\lambda_v(0)$ | $0.12921828\times 10^{1}$ |
| $\lambda_\gamma(0)$ | $-0.40492074\times 10^{-1}$ |
| $\lambda_m(0)$ | −0.68114869 |
| *Final time (scaled)* | |
| $t_1$ | $0.29808814\times 10^{2}$ |

exit, the flight-path angle in absolute values is slightly larger than in problem P1. Hence, the thrusting interval at HEO and LEO is prolongated and the fuel consumption is increased.

Because of the proper numerical treatment of the atmospheric edge, the Hamiltonian turns out to be numerically equivalent zero.

Notice that the adjoint $\lambda_v$, shown in Fig. 5, has one positive arc followed by one negative arc. The sole zero is inside the atmospheric part. Therefore, the assumption used by Mease and Vinh[15] that $\lambda_v$ has no zeros is not satisfied for the given problem.

The control variables are presented in Figs. 3 and 4. Note that Figs. 3 and 4 show the atmospheric part only. In addition, $\mathcal{H}_\eta$ is shown in Fig. 3. On bounded arcs $\mathcal{H}_\eta \geq 0$, it is necessary to fulfill the minimum principle. On arcs with unbounded $\eta$, $\mathcal{H}_\eta = 0$ has to be satisfied. The present solution meets all of these conditions. Also, the switching function of thrust $\phi$, which is shown in Fig. 4, has only two zero points, $\tau_{\zeta_1}$ and $\tau_{\zeta_2}$, as predicted. In $(0, \tau_{\zeta_1})$ and $(\tau_{\zeta_2}, 1)$, $\phi < 0$ holds.

To enable numerical comparisons, the initial values of the switching points and the adjoint variables of the solution of problem P2b are listed in Table 4.

#### Omitting Coast Subarcs

In the classical treatment of AOT problems with impulsive thrust, only the atmospheric part is considered. By the application of the conservation laws of energy and angular momentum, the states at HEO or LEO, respectively, are computed via the states at the atmospheric edge.

In the same way, the intermediate coast subarcs ($T \equiv 0$) outside atmosphere, where the trajectory of the AOTV is determined by Earth's gravitation field only, can be omitted. In this formulation, the problem consists of the two propulsion subarcs and the atmospheric part in between. At the junction points, the states have well-defined discontinuities. Also, the adjoints have to be updated. The benefit is the reduced computational effort in omitting integration intervals. On the other hand, information about thrust subarcs that might additionally arise would have been lost. Therefore, the original formulation is preferred.

## Conclusions

In this paper, a coplanar minimum-fuel AOT from geosynchronous equatorial orbit to LEO has been considered. A complex and realistic formulation of this problem including limited thrust, nonvanishing propulsion intervals, and Earth's rotation has been presented. The resulting optimal control problem has been solved numerically with an indirect method.

The results show that the optimal control structure for the lift coefficient consists of one bounded, that is, one minimal, and one free arc. The control sequence of the thrust is maximal–minimal–maximal. Investigations of the thrust switching function do not reveal a third propulsion arc during the transfer.

The impulsive thrust trajectories are approximated by a high thrust limit. Varying the maximum magnitude of thrust has significant consequences on the flight path, mainly outside the atmosphere. Whereas in high-thrust-limit trajectories the vehicle immediately decreases the altitude, in the low thrust case the altitude is slightly increased first and afterward reduced. Therefore, the trajectory and the total time of the transfer are extended. Also, the fuel consumption is increased about 0.2%. The extension of the thrust arcs implies changes to the flight-path angle, also inside the atmosphere. However, the time of passing the atmosphere remains almost identical.

Taking into account Earth's rotation, the trajectory inside the atmosphere is mainly afflicted. Because the velocity of the vehicle subject to the now rotating atmosphere is decreased, aerodynamic forces are reduced also. To compensate this disadvantage, the vehicle attains a lower minimum altitude and remains inside the atmosphere for a longer time. The parts outside the atmosphere are not altered significantly. Therefore, the thrust arcs and the fuel consumption are only slightly increased.

## Acknowledgment

This research was supported by Deutsche Forschungsgemeinschaft Contract Ob98/2-1.

## References

[1]London, H. S., "Change of Satellite Orbit Plane by Aerodynamic Maneuvering," *Journal of the Aerospace Sciences*, Vol. 29, 1962, pp. 323–332.

[2]Walberg, G. D., "Survey of Aeroassisted Orbit Transfer," *Journal of Spacecraft and Rockets*, Vol. 22, No. 1, 1985, pp. 3–18.

[3]Mease, K. D., "Optimization of Aeroassisted Orbit Transfer: Current Status," *Journal of Astronautical Sciences*, Vol. 36, Nos. 1/2, 1988, pp. 7–33.

[4]Miele, A., "Recent Advances in the Optimization and Guidance of Aeroassisted Orbital Transfer, First John V. Breakwell Memorial Lecture," *Acta Astronautica*, Vol. 38, No. 10, 1996, pp. 747–768.

[5]Miele, A., and Venkataraman, P., "Optimal Trajectories for Aeroassisted Orbital Transfer," *Acta Astronautica*, Vol. 11, Nos. 7/8, 1984, pp. 423–433.

[6]Naidu, D., *Aeroassisted Orbital Transfer*, Springer-Verlag, Berlin, 1994, Chaps. 2, 3.

[7]Miele, A., Wang, T., and Deaton, A. W., "Properties of the Optimal Trajectories for Coplanar, Aeroassisted Orbital Transfer," *Journal of Optimization Theory and Applications*, Vol. 69, No. 1, 1991, pp. 1–30.

[8]Dickmann, E. D., "The Effect of Finite Thrust and Heating Constraints on the Synergetic Plane Change Maneuver for a Space Shuttle Orbiter-Class Vehicle," NASA TN D-7211, Oct. 1973.

[9]Zimmermann, F., and Calise, A., "Numerical Optimization Study of Aeroassisted Orbital Transfer," *Journal of Guidance, Control, and Dynamics*, Vol. 21, No. 1, 1998, pp. 127–133.

[10]Seywald, H., "Variational Solutions for the Heat-Rated-Limited Aeroassisted Orbital Transfer Problem," *Journal of Guidance, Control, and Dynamics*, Vol. 19, No. 3, 1996, pp. 686–692.

[11]Baumann, H., and Oberle, H. J., "Numerical Computation of Optimal Trajectories for Coplanar, Aeroassisted Orbital Transfer," *Hamburger Beiträge zur Angewandten Mathematik*, Reihe A, Preprints, Hamburg, Germany, Dec. 1999.

[12]Miele, A., Basapur, V. K., and Lee, W. Y., "Optimal Trajectories for Aeroassisted, Noncoplanar Orbital Transfer," *Acta Astronautica*, Vol. 15, Nos. 6/7, 1987, pp. 199–411.

[13]Horie, K., and Conway, B., "Optimal Aeroassisted Orbital Interception," *Journal of Guidance, Control, and Dynamics*, Vol. 22, No. 5, 1999, pp. 625–631.

[14]Bryson, A. E., and Ho, Y. C., *Applied Optimal Control,* Ginn, Walham, MA, 1969, Chap. 3.

[15]Mease, K. D., and Vinh, N. X., "Minimum-Fuel Aeroassisted Coplanar Orbit Transfer Using Lift Modulation," *Journal of Guidance, Control, and Dynamics*, Vol. 8, No. 1, 1985, pp. 134–141.

[16]Oberle, H. J., and Taubert, K., "Existence and Multiple Solutions of the Minimum-Fuel Orbit Transfer Problem," *Journal of Optimization Theory and Applications*, Vol. 95, No. 2, 1997, pp. 243–262.

[17]Bulirsch, R., "Die Mehrzielmethode zur Numerischen Lösung von Nichtlinearen Randwertaufgaben und Aufgaben der Optimalen Steuerung," Rept., Carl–Cranz–Gesellschaft, Oberpfaffenhofen, Germany, 1971.

[18]Stoer, J., and Bulirsch, R., *Introduction to Numerical Analysis,* 2nd ed., corrected 3rd print, Texts in Applied Mathematics, Springer, New York, Vol. 12, 1996, Chap. 7.

[19]Oberle, H. J., and Grimm, W., "BNDSCO—A Program for the Numerical Solution of Optimal Control Problems," Rept. 515, Inst. for Flight Systems Dynamics, German Aerospace Research Establishment, Oberpfaffenhofen, Germany, 1989.